A Mesoporous, Silica-Immobilized-Nanoparticle Colorimetric Chemosensor for the Detection of Nerve Agents

Hyun Jung Kim, Ji Ha Lee, Hyejin Lee, Jae Hong Lee, Joung Hae Lee, Jong Hwa Jung, and Jong Seung Kim**

A new and an easy-to-make colorimetric azo-pyridine, 1, and its recyclable mesoporous silica-immobilized nanoparticles for nerve-agent detection are synthesized. The binding site, comprising an azo-pyridine moiety, is capable of selectively sensing diethylchlorophosphate (DCP), one of the nerve-agent mimics of chemical-warfare agents, over a series of other phosphate compounds. Compound 1 shows ratiometric changes in absorption spectroscopy to the extent of a 60 nm red-shift upon the addition of DCP, mainly due to a change in the intramolecular charge transfer (ICT) in 1. The color change of receptor 1 from yellow to red in the concentration region $\approx 1.0 \times 10^{-6}$ M is sufficient for the selective detection of the DCP nerve-agent mimic by the naked eye. With regards to solid-phase application, mesoporous silica nanoparticles using 1 (MSIAP) are also prepared using a sol-gel grafting reaction. The color of the MSIAP also changes from red to yellow when dipped into an aqueous DCP solution, and turns back to red when treated with NaOH solution, with non-toxic diethylphosphoric acid being given off. The absorption changes of MSIAP in the presence of DCP are consistent within the 3–9 pH range.

1. Introduction

A chemical warfare agent is a substance "intended for use in military operations to kill, seriously injure, or incapacitate man because of its physiological effects." In the modern era, chemical-warfare agents have been divided into five categories: nerve agents, vesicants, choking agents, blood agents, and incapacitants.[1,2] The development of chemical-warfare agents during the Second World War led to the so-called "nerve agents", which are fast-acting poisons that attack the nervous system. Among chemical-warfare agents, nerve agents are extremely dangerous and their high toxicity and ease of production underscore the need to detect these lethal chemicals via quick and reliable procedures.[1,2]

Nerve agents, a class of phosphorus-containing organic chemicals that disrupt the mechanism by which nerves transfer messages to organs, have been studied extensively due to their rapid and severe effects on human- and animal-health systems.[3] Up to now, many detection methods for nerve agents have been developed based on fluorogenic, colorimetric, and enzymatic methods.[4,5] Nevertheless, these methods suffer from some limitations, such as slow response, lack of specificity, limited selectivity, low sensitivity, difficulties in real-time monitoring, and water solubility.[4,5] In particular, since the nerve-agent mimic is easily hydrolyzed in water within a few minutes, non-aqueous solutions should be used in most cases for the detection of nerve agents, in order to look at absorption and emission spectrophotometric changes, which greatly limits analytical application in real samples.[4,5] Therefore, simple and efficient detection methods for nerve agents in water media remain of great interest these days.

Silica-based nanoparticles are of great interest for biomedical- and environmental-research applications such as bioseparation, drug targeting, cell isolation, enzyme immobilization, and protein purification because of their biocompatibility and stability against degradation.[6–10] It is clear that receptor-immobilized nanoparticles have some important advantages as solid chemosensors. Firstly, such nanoparticles are readily synthesized by sol-gel condensation, a versatile technique that permits the presence of chemical functionalities. Secondly, immobilized receptors on an inorganic support can remove guest molecules (toxic metal ions and anions) from the pollutant solution. Thirdly, the nanoparticles can be easily isolated from pollutants by filtration and repeatedly utilized with suitable treatment. In this aspect, the homogeneous porosity and large surface area of mesoporous silicas (SBA-15 and MCM-41) make them promising as inorganic supports.[11–14] If hybrid nanomaterials can

H. J. Kim, J. H. Lee, J. S. Kim
Department of Chemistry
Korea University
Seoul 136-701, Korea
E-mail: jongskim@korea.ac.kr
J. H. Lee, H. Lee, J. H. Jung
Department of Chemistry and Research Institute of Natural Science
Gyeongsang National University
Jinju 660-701, Korea
E-mail: jonghwa@gnu.ac.kr
J. H. Lee
Korea Research Institute of Standards and Science
Daejon 305-600, Korea

DOI: 10.1002/adfm.201100968

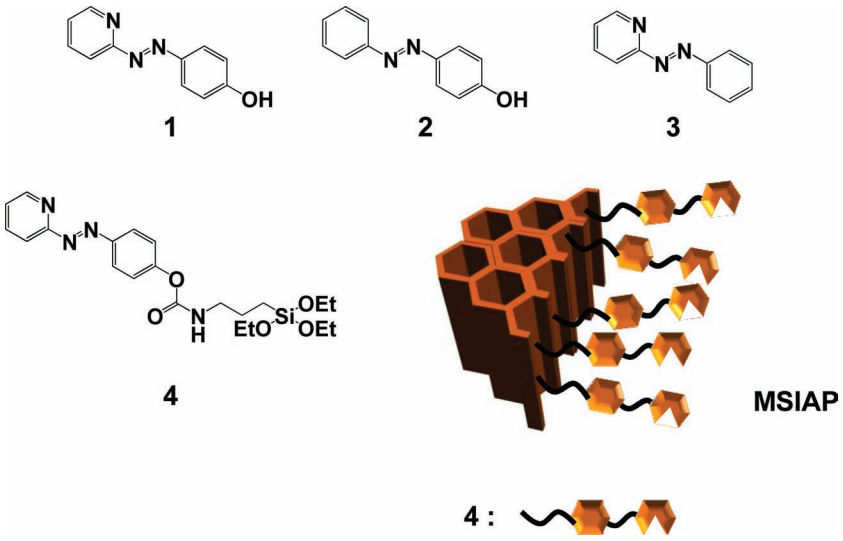

Scheme 1. Chemical structures of **1–4** and MSIAP.

be provided as portable systems for chemosensors,[15] silica-based hybrid nanoamaterials will be easily able to detect specific guest molecules in biological and environmental fields, and thus could be utilized as recyclable sensors.

We have investigated a method of detecting nerve agents by using a nerve-agent mimic, diethylchlorophosphate (DCP), which functions as an acetylcholinesterase inhibitor, but which is rather less harmful to the human body than real nerve agants.[5d] In real nerve agents, this inhibition has been known to lead to paralysis and death.[3] The desired probe for DCP would therefore be selectively unresponsive to much-less-harmful agents that lack reactive acyl or phosphoryl halide groups, such as pinacolylmethylphosphonate (PMP), dimethyl-methyl phosphonate (DMMP), triethylphosphate (TEP) and tributylphosphate (TBP).

Herein we present a synthesis of azo-pyridine (**1**), which contains a colorimetric mesoporous silica-immobilized chemosensor, and its highly selective UV–vis spectrophotometric changes, along with changes detectable by the naked-eye for DCP. The organic-inorganic hybrid mesoporous silica-immobilized azo-pyridine based on **1** (MSIAP) that we have developed is the first recyclable colorimetric sensor that can be used in 100% aqueous solution for DCP sensing.

2. Results and Discussion

Azo-compound **1**[16] was prepared by the reaction of 2-hydrazinopyridine with 1,4-benzoquinone in acidic media. Reference compounds **2**[17] and **3**[18] were also prepared using literature procedures reported previously. Compound **4** was also prepared by the reaction of **1** with 3-triethoxysilylpropylisocyanate in CH_3CN. Subsequently, MSIAP was synthesized by coupling **4** with mesoporous silica in toluene. All of the chemical structures of **1–4** and MSIAP (**Scheme 1**) were confirmed by ^{1}H-NMR spectroscopy, ^{13}C-NMR spectroscopy, and fast-atom-bombardment mass spectrometry (FAB-MS) (see Supporting Information).

As a first step, the reactivity of **1** with DCP, PMP, DMMP, TEP, and TBP in acetonitrile was tested. These organophosphates have been widely used as simulants, as they display reactivities similar to those of nerve agents such as Tabun, Sarin and Soman, yet they lack their toxicity.[3]

The absorption spectra of the stable *trans* isomers of the azo-pyridine chemosensor, **1**, exhibit an intense peak at 345 nm (ε = 2.3×10^4 M^{-1} cm^{-1}), which corresponds to the π–π^* transition.[16] Upon addition of 10 equiv of DCP to a solution of **1**, the absorption band was red-shifted to 405 nm (ε = 2.5×10^4 M^{-1} cm^{-1}), which resulted in a modulation from yellow to red in organic media (**Figure 1**a). This spectroscopic-change event is obviously due to enhanced intramolecular charge transfer (ICT). The enhancing ICT,

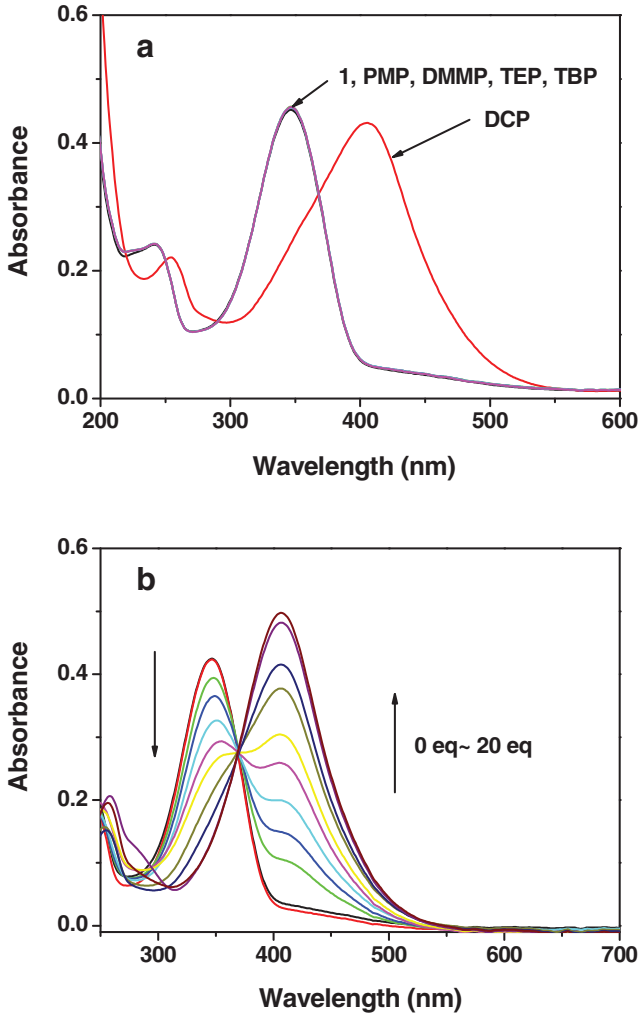

Figure 1. a) UV–vis spectra of **1** (20.0×10^{-6} M) upon addition of DCP, PMP, DMMP, TEP, and TBP (10 equiv) in CH_3CN. b) UV–vis titration spectra of **1** (20.0×10^{-6} M) upon addition of various amounts of DCP in CH_3CN.

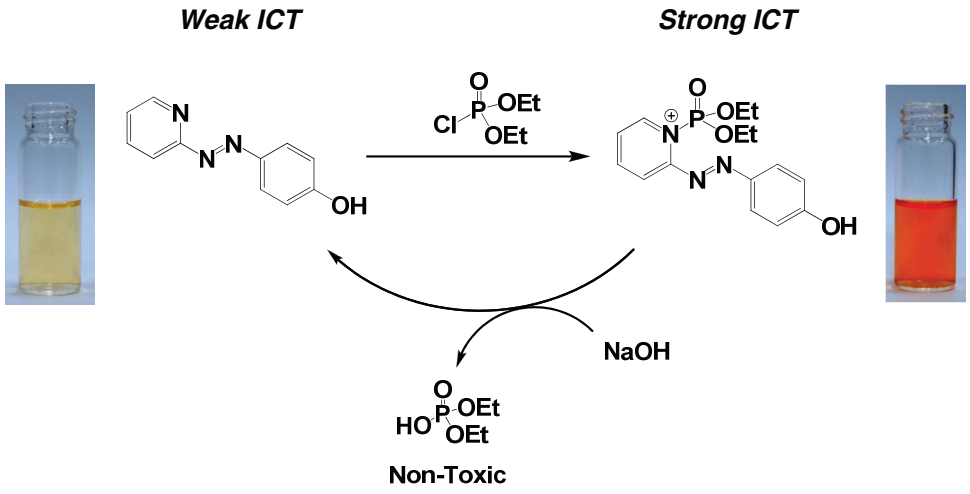

Scheme 2. Proposed mechanism of ICT change of **1** in DCP sensing.

promoted by the strong *push-pull* effect between the electron-donating oxygen (OH) and the electron-accepting pyridinium group,[19] exerts a 60 nm bathochromic shift of the maximum wavelength in the UV–vis spectrum. Figure 1b gives the detailed absorption changes of **1** upon gradual titration of DCP (0–20 equiv) (**Scheme 2**).

In acidic solution, **1** showed a strong absorption band centered at 405 nm, as seen in Figure S1, Supporting Information, which supports the notion that the formation of the pyridinium ion of **1** enhances the ICT when it reacts with DCP. The new band at 405 nm is also similar to that of a 2-pyridine nitrogen, methylated azo compound that was previously reported by Velasco et al.[16]

To elucidate the role of the pyridine nitrogen atom in the nucleophilic interaction with **1** on the ICT development, we synthesized two structural analogues, **2** and **3**. We found however that **2** did not show any spectral changes on DCP addition, implying the DCP binding to **1** is dominated by the presence of the pyridine nitrogen atom not by the phenolic OH group. Compound **3**, which does not have an electron-donating group such as OH, showed smaller spectral changes (20 nm) in the presence of DCP than **1** (Figure S2, Supporting Information); this firmly demonstrates that the *push-pull*-mediated ICT from the OH to the pyridine N atom is of critical importance in DCP detection.

The 1:1 binding was evidenced by a peak at m/z = 337.2 (calcd 337.12), corresponding to $[\mathbf{1} + \text{DCP} + \text{H}]^{2+}$ in the electrospray-ionization mass-spectrometry (ESI-MS) spectrum of a mixture of **1** and 20×10^{-6} M DCP (Figure S3, Supporting Information).

It is well known that strong bases such as NaOH can react with phosphates (DCP or DFP) to make a less-toxic hydrolysis product (phosphoric acid).[20] From the absorbance changes and color revival from red to yellow, we also confirmed that the dissociation of DCP from the **1**-DCP complex occurs easily with NaOH treatment, to return to the original **1**, making the compound recyclable (**Figure 2**).

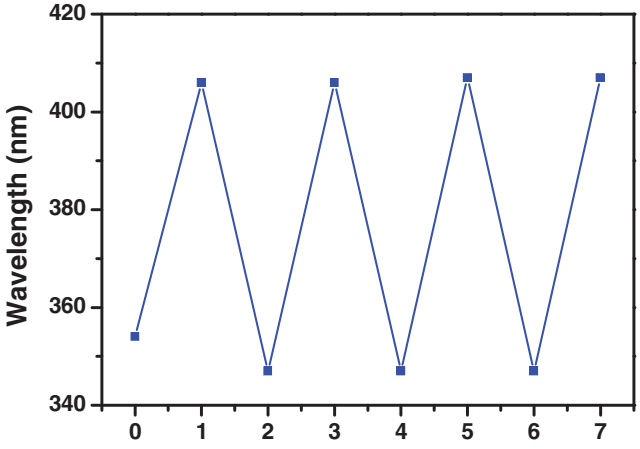

Figure 2. Plot for the absorbance of MSIAP by alternated dipping in a 1.0×10^{-6} M aqueous solution of DCP and 10.0×10^{-6} M NaOH treatment. The cyclic index is the number of alternating dipping/rinsing cycles, with the vertical axis showing the absorbance for the MSIAP at 405 nm.

In consideration of extending its usefulness, MSIAP was fabricated by a sol-gel reaction of **4** with mesoporous silica. Immobilization of the receptor **4** was conducted under reflux conditions for 24 h in toluene to give the MSIAP. In this process, the triethoxylsilyl group of **4** undergoes hydrolysis and covalently attaches to the surface of the mesoporous silica. After cooling to room temperature, the red solid product was filtered, washed with tetrahydrofuran (THF), and then dried overnight. The MSIAP was characterized by transmission electron microscopy (TEM), Fourier transform IR (FTIR) spectroscopy, Brunauer–Emmett–Teller (BET) isotherms, time-of-flight secondary-ion mass spectrometry (TOF-SIMS), and X-ray photoelectron spectroscopy (XPS).

In **Figure 3**, the TEM picture of MSIAP clearly shows the formation of a well-ordered hexagonal arrangement of mesoporous channels after attaching **4**. To investigate the porosity changes

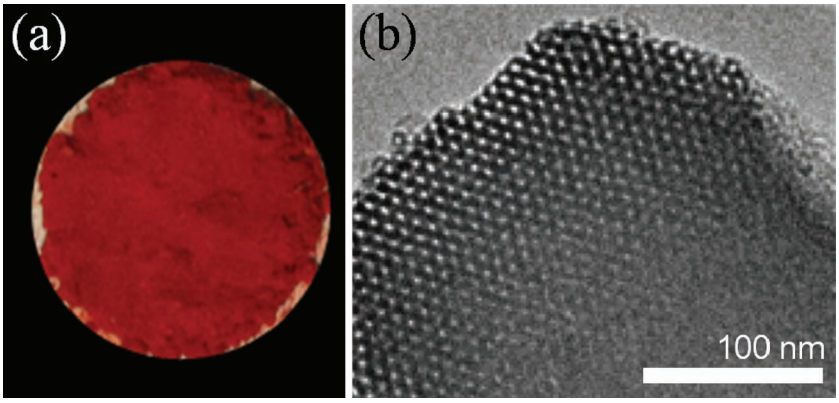

Figure 3. a) Photograph of the MSIAP. b) TEM image of the MSIAP.

of the mesoporous silica induced by the introduction of **4**, we measured the surface areas, pore volumes, and pore diameters of both the mesoporous silica and the MSIAP by way of their nitrogen adsorption-desorption isotherms (Figure S4, Supporting Information). The mesoporous silica had a BET surface area of 1050.8 $m^2\ g^{-1}$ and a pore volume of 0.47 $cm^3\ g^{-1}$. On the other hand, we observed that the MSIAP had a BET surface area of 850.35 $m^2\ g^{-1}$ and a pore volume of 0.32 $cm^3\ g^{-1}$. The mesoporous silica and the MSIAP had Barrett–Joyner–Halenda (BJH) pore diameters of 8.53 and 7.20 nm, respectively. The decreased surface area and pore diameter in MSIAP are attributable to the attachment of **4** to the mesoporous silica (Figure S4, Supporting Information).

Moreover, for further structural proof of the MSIAP, IR spectroscopy for both mesoporous silica and MSIAP was performed. For the mesoporous-silica nanoparticles, IR peaks appeared at 3450, 1658, and 1084 cm^{-1}, whereas peaks appeared at 3010, 2976, 2933, 1646, 1633, 1540, 1471, 1446, 1428, and 1382 cm^{-1} for the MSIAP (Figure S5, Supporting Information), with the new peaks originating from the azo-pyridine, **4**, giving solid evidence that **4** was attached to the surface of the mesoporous silica.

The TOF-SIMS spectrum of the MSIAP displayed fragments of **4**-3OEt + 3H (m/z = 316), thereby providing a proof that **4**-3OEt + 3H was anchored onto the surface of the silica particles (Figure S6, Supporting Information). The mesoporous-silica nanoparticles before and after functionalization of **4** were further confirmed by XPS (Figure S7, Supporting Information). The XPS spectrum of the mesoporous-silica nanopaticles before immobilization of **4** showed the Si_{2P} and O_{1S} binding energies (Figure S7a, Supporting Information), whereas the C_{1S} and N_{1S} binding energies for carbon and nitrogen, respectively, appeared for MSIAP (Figure S7b, Supporting Information). We further measured the TGA thermogram of MSIAP. The TGA results (Figure S8, Supporting Information) showed that the MSIAP consisted of only 35.5 wt% of receptor **4**.

Nerve-agent-sensor development under aqueous conditions is hampered by the instability of suitable chloride-containing electrophiles (DCP is hydrolyzed in water buffered to a pH of 7 within a few minutes). An important advantage of the MSIAP in our study is that it is more practically accessable: it is a 100%-water-soluble and recyclable nerve-agent detector. In the absence of nerve-agent simulants, a suspension of MSIAP in water was initially red in color. In the presence of DCP, however, the suspension of MSIAP showed a color change from red to yellow. On the other hand, no significant changes in absorption were observed in parallel experiments with PMP, DMMP, TEP, and TBP (**Figure 4**). From these spectroscopic changes, we noticed that the MSIAP reveals a high selectivity for DCP, showing a similar spectroscopic response to that of **1**, mentioned eariler. The results imply that the MSIAP is considerably applicable to the environmental field as a new organic-inorganic hybrid sensor for the detection of the nerve agent, DCP. An evaluation of the time course for the absorption change of MSIAP at 405 nm (Figure S9, Supporting Information) indicates that immediately after the addition of DCP, the absorption intensity of MSIAP starts to increase and that, by 30 s, the absorption intensity is almost saturated. That is, this fast response time makes it a rapid and convenient method for the quantification of DCP in aqueous solution.

In order to extend the above performance to a portable chemosensor kit, a disk-type pellet was prepared from MSIAP (**Figure 5**). The red color of the disk-type pellet of MSIAP changed to yellow when dipped in DCP (10×10^{-6} M) aqueous solution. On the other hand, no significant changes in absorption were observed in parallel experiments in the cases of PMP,

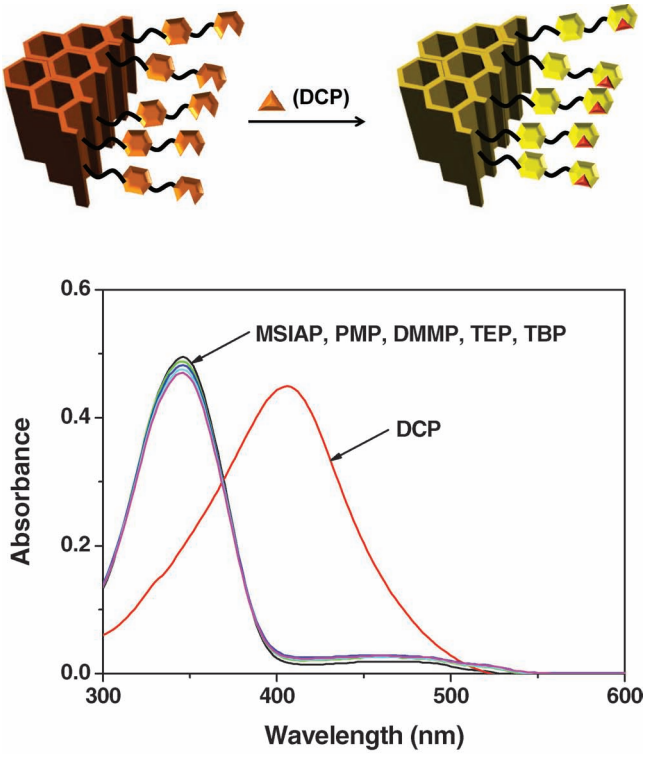

Figure 4. UV–vis spectra of MSIAP (20.0×10^{-6} M) upon addition of DCP, PMP, DMMP, TEP, and TBP (10 equiv) in H_2O.

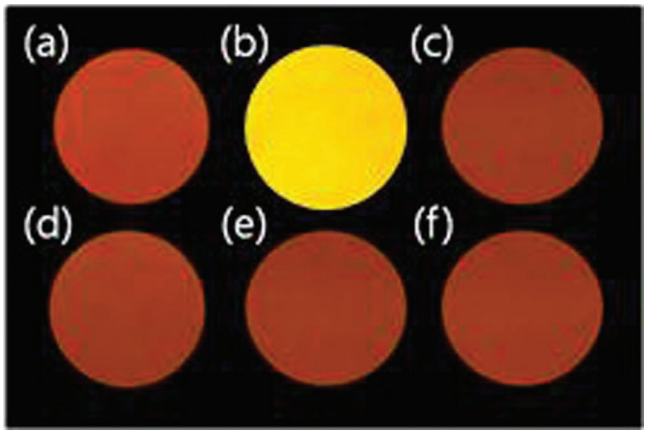

Figure 5. Photogram of MSIAP (10 mg) (a), and the MSIAP in the presence of DCP (b), DMP (c), DMMP (d), TEP (e), and TBP (f) (10 equiv).

DMMP, TEP, and TBP solutions (10×10^{-6} M). In addition, the solid fluorescence spectrum of the disk-type pellet of MSIAP with DCP was the same as that obtained from MSIAP dispersed in aqueous solution. The fluorescence change was found to be fully reversible when the disk-type pellet prepared from MSIAP was rinsed using NaOH (10×10^{-6} M) solution. This result implies that the disk-type pellet prepared from MSIAP is applicable as a portable chemosensor for the detection of DCP in the biological and environmental fields.

The highly selective DCP recognition of MSIAP demonstrates that the approach employed in the present study is capable of co-operatively enhancing and controlling the selectivity towards DCP. More importantly, quantitative measurements of the absorption maximum of DCP-bound MSIAP indicate that the absorption change correlates linearly with the [DCP] over the 17–84 ppb range investigated (Figure S10, Supporting Information). We determined that the detection limit of MSIAP for DCP is 0.53 ppb.

We have also investigated the effect of pH on the spectrophotometric behaviour of MSIAP in both the absence and the presence of DCP, because, ideally for biological and environmental applications, sensing should be practical over a range of pH values. Over the pH range from 3 to 9, MSIAP showed no absorption in the absence of DCP, whereas upon addition of DCP, MSIAP displayed almost equal absorption intensities at all pH values investigated within this range. These results clearly confirm the suitability of MSIAP for use in physiological environments spanning the 3–9 pH range (Figure S11, Supporting Information).

3. Conclusions

We synthesized chromogenic azo-pyridine (**1**) and its recyclable MSIAP for the detection of the nerve-agent DCP. The MSIAP shows a high sensitivity and selectivity for DCP over other organophosphorus compounds, with respect to absorption changes in 100% aqueous solution, and the corresponding color changes are easily recognizable by the naked-eye. Moreover, MSIAP not only detects the toxins, but can simultaneously decompose them to less-toxic molecules after treatment with NaOH, and then turns back to the original, recyclable MSIAP. The azo-pyridine motif, as an ICT framework for DCP sensing, is a new field and other nerve-agent sensors can be easily designed based on the present article as well.

4. Experimental Section

Instruments and Reagents: The UV–vis absorption spectra were recorded using a Sinco S-3100 spectrophotometer. The NMR and mass spectra were recorded using a Varian (400 MHz) NMR spectrometer and a JMS-700 MStation mass spectrometer, respectively. The TEM images were captured using a JEOL JEM-2100 F microscope. The nitrogen-adsorption isotherms were measured at 78 K using a Micromeritics ASAP 2010 analyzer. TOF-SIMS was performed using a Model PHI 7200 instrument equipped with Cs- and Ga-ion guns for positive- and negative-ion mass detection. The XPS spectra were recorded using a Thermo VG Scientific spectrometer.

The reactants, 2-hydrazinopyridine, 1,4-benzoquinone, phenol, sodium nitrite, aniline, and the organophorphorus compounds of DCP, PMP, DMMP, TEP, and TBP were purchased from Aldrich and used as received. All of the solvents were analytical-reagent-grade chemicals from Duksan Pure Chemical Co., Ltd. For the absorbance spectra, the MeCN used was HPLC-reagent grade.

Preparation of ***4***: Under nitrogen, a solution of **1** (0.1 g, 0.5 mmol) and 3-triethoxysilylpropylisocyanate (0.125 g, 0.5 mmol) was suspended in dry $CHCl_3$ (10 mL). Et_3N (10 mL) was then added and the mixture was refluxed under N_2 for 48 h. The mixture was evaporated by rotary evaporation and the crude product was purified by column chromatography (silica, ethyl acetate/hexane 1:4) to give 0.2 g of **4** (89% yield).

^{1}H NMR (400 MHz, $CDCl_3$, δ): 8.70 (d, J = 4.8 Hz, 1H), 8.04 (d, J = 8.9 Hz, 2H), 7.86 (t, J = 8.0 Hz, 1H), 7.78 (d, J = 8.0 Hz, 1H), 7.37 (t, J = 4.8 Hz, 1H), 7.28 (d, J = 8.8 Hz, 2H), 5.65 (t, J = 5.8 Hz, 1H), 3.76 (q, 6H), 3.23 (q, 2H), 1.67 (q, 2H), 1.22 (t, J = 8.2 Hz, 9H), 0.68 (t, J = 8.2 Hz, 2H); ^{13}C NMR (100 MHz, $CDCl_3$, δ): 162.9, 154.4, 154.1, 149.6, 138.6, 125.1, 125.0, 122.3, 115.7, 58.7, 43.8, 31.8, 23.2, 18.5, 14.3, 7.9; FAB-MS (m/z): $[M + H]^+$ calcd for $C_{21}H_{31}N_4O_5Si$, 447.58; found 447.3.

Preparation of Mesoporous Silica: Mesoporous silica was synthesized starting from the preparation of a hydrochloric acid solution of poly(ethylene oxide)-*block*-poly(propylene oxide)-*block*-poly(ethylene oxide) triblock copolymer (P-123). Tetraethyl orthosilicate (TEOS) was then added and the mixture was stirred at 40 °C for 20 h. The molar composition was 1:5.9:193:0.017 TEOS:HCl:H_2O:P-123. The solid was aged at 65 °C for 1 d and was then filtered, washed and dried at 90 °C. To cleave the template to generate the mesopores, 1.0 g of the as-synthesized SBA-15 silica was mixed with 100 mL of 60 wt% H_2SO_4 solution and refluxed at 95 °C for 1 d. The product was recovered by washing with water and was dried at 90 °C. To generate the mesopores, the acid-treated sample was heated to 200 °C in air. To remove any cationic surfactants from the resulting dried, fiber-like flocculates and particles, the sample was calcined in a box furnace in air at 500 °C for 5 h, at a ramp rate of 1 °C min^{-1}.

Immobilization of Receptor ***4*** *onto Mesoporous Silica*: Compound **4** (100 mg) was dissolved in toluene (10 mL). The mesoporous silica (100 mg) was added as a solid. The suspension of silica was stirred under reflux conditions for 24 h in toluene. Then, the collected solid was washed copiously with toluene (50 mL) to rinse away any surplus **4** and dried under vacuum.

Supporting Information

Supporting Information is available from the Wiley Online Library or from the author.

Acknowledgements

This work was supported by a grant from the CRI program (No. 2011-0000420) (J.S.K.) and World Class University (WCU) Program (R32-2008-000-20003-0) (J.H.J.) from the National Research Foundation of Korea.

Received: May 3, 2011
Published online: September 9, 2011

[1] O. A. Sadik, W. H. Land, J. Wang, *Electroanalysis* **2003**, *15*, 1149.
[2] a) W. S. Augerson, *Chemical and Biological Warfare Agents*, *A Review of the Scientific Literature as it Pertains to Gulf War Illnesses*, *Vol. 5*, RAND, Santa Monica, CA **2000**; b) D. R. Walt, D. R. Franz, *Anal. Chem.* **2000**, *72*, 738A.
[3] a) A. Silver, *The Biology of Cholinesterases*, Elsevier, New York **1974**, p 449; b) *Goodman and Gilman's The Pharmacological Basis of Therapeutics*, 10th ed. (Eds: J. G. Hardman, L. E. Limbird, A. Goodman Gilman), McGraw–Hill, New York **2001**.
[4] a) B. Gehauf, J. Goldenson, *Anal. Chem.* **1957**, *29*, 276; b) S.-W. Zhang, T. M. Swager, *J. Am. Chem. Soc.* **2003**, *125*, 340; c) T. J. Dale, J. Rebek, Jr., *J. Am. Chem. Soc.* **2006**, *128*, 4500; d) F. Ilhan, D. S. Tyson, M. A. Meador, *Chem. Mater.* **2004**, *16*, 2978; e) S. Bencic-Nagale, T. Sternfeld, D. R. Walt, *J. Am. Chem. Soc.* **2006**, *128*, 5041; f) T. J. Dale, J. Rebek Jr., *Angew. Chem. Int. Ed.* **2009**, *48*, 7850.
[5] a) K. J. Wallace, J. Morey, V. M. Lynch, E. V. Anslyn, *New J. Chem.* **2005**, *29*, 1469; b) K. J. Wallace, R. I. Fagbemi, F. J. Folmer-Andersen, J. Morey, V. M. Lynch, E. V. Anslyn, *Chem. Commun.* **2006**, 3886; c) H. Y. Tan, N.-T. Nguyen, W. K. Loke, Y. T. Tan, in *Biomedical Applications of Micro- and Nanoengineering III* (Ed: D. V. Nicolau) SPIE, Bellingham, WA, **2006** (*Proc. SPIE* **2006**, *6416*, 64160M); d) E. R. Menzel, L. W. Menzel, J. R. Schwierking, *Talanta* **2005**, *67*, 383.
[6] S. A. El-Safty, D. Prabhakaran, A. A. Ismail, H. Matsunaga, F. Mizukami, *Chem. Mater.* **2008**, *20*, 2644.
[7] R. Chen, R. P. J. Bronge, P. C. J. Kamer, P. W. N. M. van Leeuwen, J. N. H. Reek, *J. Am. Chem. Soc.* **2004**, *126*, 14557.
[8] a) M. Park, S. Seo, I. S. Lee, J. H. Jung, *Chem. Commun.* **2010**, 4478; b) T. Balaji, S. A. El-Safty, H. Matsunaga, T. Hanaoka, F. Mizukami, *Angew. Chem. Int. Ed.* **2006**, *45*, 7202.
[9] a) H. Son, H. Y. Lee, J. M. Lim, D. Kang, W. S. Han, S. S. Lee, J. H. Jung, *Chem. Eur. J.* **2010**, *16*, 11549; b) H. Y. Lee, D. R. Bae, J. C. Park, H. Song, W. S. Han, J. H. Jung, *Angew. Chem. Int. Ed.* **2009**, *48*, 1239; c) H. J. Kim, S. J. Lee, S. Y. Park, J. H. Jung, J. S. Kim, *Adv. Mater.* **2008**, *20*, 3229.
[10] a) S. Angelos, E. Johansson, J. F. Stoddart, J. I. Zink, *Adv. Funct. Mater.* **2007**, *17*, 2261; b) S. Saha, K. C.-F. Leung, T. D. Nguyen, J. F. Stoddart, J. I. Zink, *Adv. Funct. Mater.* **2007**, *17*, 685.
[11] W. S. Han, H. Y. Lee, S. H. Jung, S. J. Lee, J. H. Jung, *Chem. Soc. Rev.* **2009**, *38*, 1904.
[12] J. H. Jung, M. Park, S. Shinkai, *Chem. Soc. Rev.* **2010**, *39*, 4286.
[13] F. Hoffmann, M. Cornelius, J. Morell, M. Froba, *Angew. Chem. Int. Ed.* **2006**, *45*, 3216.
[14] R. Martínez-Máñez, F. Sancenon, *Coord. Chem. Rev.* **2006**, *250*, 3081.
[15] a) H. S. Jung, P. S. Kwon, J. W. Lee, J. I. Kim, C. S. Hong, J. W. Kim, S. Yan, J. Y. Lee, J. H. Lee, T. Joo, J. S. Kim, *J. Am. Chem. Soc.* **2009**, *131*, 2008; b) S. K. Kim, S. H. Kim, H. J. Kim, S. H. Lee, S. W. Lee, J. Ko, R. A. Bartsch, J. S. Kim, *Inorg. Chem.* **2005**, *44*, 7866; c) H. J. Kim, J. Hong, A. Hong, S. Ham, J. H. Lee, J. S. Kim, *Org. Lett.* **2008**, *10*, 1963; d) M. H. Lee, H. J. Kim, S. Yoon, N. Park, J. S. Kim, *Org. Lett.* **2008**, *10*, 213; e) H. J. Kim, S. K. Kim, J. Y. Lee, J. S. Kim, *J. Org. Chem.* **2006**, *71*, 6611.
[16] J. Garcia-Amorós, W. A. Massad, S. Nonell, D. Velasco, *Org. Lett.* **2010**, *12*, 3514.
[17] H. Xu, X. Zeng, *Bioorg. Med. Chem. Lett.* **2010**, *20*, 4193.
[18] N. D. Paul, T. Krämer, J. E. McGrady, S. Goswami, *Chem. Commun.* **2010**, 7124.
[19] G. K. B. Clentsmith, V. C. Gibson, P. B. Hitchcock, B. S. Kimberley, C. W. Rees, *Chem. Commun.* **2002**, 1498.
[20] Y.-C. Yang, J. A. Baker, R. J. Ward, *Chem. Rev.* **1992**, *92*, 1729.